ELSEVIER

Journal of Neuroscience Methods 51 (1994) 95–106

JOURNAL OF NEUROSCIENCE METHODS

Multi-neuronal signals from the retina: acquisition and analysis

Markus Meister [a,*], Jerome Pine [b], Denis A. Baylor [c]

[a] *Department of Cellular and Developmental Biology, Harvard University, Cambridge, MA 02138, USA;* [b] *Department of Physics, California Institute of Technology, Pasadena, CA 91125, USA;* [c] *Department of Neurobiology, Stanford University School of Medicine, Stanford, CA 94305, USA*

(Received 14 January 1993; accepted 7 October 1993)

Abstract

Throughout the central nervous system, information about the outside world is represented collectively by large groups of cells, often arranged in a series of 2-dimensional maps connected by tracts with many fibers. To understand how such a circuit encodes and processes information, one must simultaneously observe the signals carried by many of its cells. This article describes a new method for monitoring the simultaneous electrical activity of many neurons in a functioning piece of retina. Extracellular action potentials are recorded with a planar array of 61 microelectrodes, which provides a natural match to the flat mosaic of retinal ganglion cells. The voltage signals are processed in real time to extract the spike trains from up to 100 neurons. We also present a method of visual stimulation and data analysis that allows a rapid characterization of each neuron's visual response properties. A randomly flickering display is used to elicit spike trains from the ganglion cell population. Analysis of the correlations between each spike train and the flicker stimulus results in a simple description of each ganglion cell's functional properties. The combination of these tools will allow detailed study of how the population of optic nerve fibers encodes a visual scene.

Key words: Retina; Ganglion cell; Optic nerve; Action potential; Multi-neuronal signaling; Electrode array

1. Introduction

1.1. Retina

The vertebrate retina is a layered neural network, about 200 μm thick, that lines the posterior half of the eyeball (Rodieck, 1973; Levick and Dvorak, 1986; Dowling, 1987). It converts the visual image generated by the eye's optics into a pattern of neural activity, processes this signal to extract certain features of interest to the organism, and transmits the result of these computations through the optic nerve to the brain. The retina contains 5 major types of neurons (Fig. 1). The rod and cone photoreceptors are connected to bipolar cells as well as horizontal cells. Bipolar cells, in turn, make synapses with amacrine cells and retinal ganglion cells, whose axons form the optic nerve. Information flowing through the network in the vertical direction, from photoreceptors through bipolar cells to retinal ganglion cells, is modified by lateral interactions mediated by the horizontal and amacrine cells.

The retina offers several advantages for the study of neural processing. It constitutes a well-defined neural circuit the general function of which is well known. It can be removed from the eye without damage to internal connections, and continues to function in vitro for many hours. The retina's natural input, a pattern of light, is easily controlled. The retina also generates a clearly defined output, namely action potentials in the ganglion cell axons, which form the optic nerve. While these features have made the retina a favorite object of neurophysiological investigations, most of the work up to now has focused on the properties of individual neurons. However, even local visual processing involves the interaction of a large number of retinal neurons. The result of these operations is transmitted to the brain in a massively parallel form: the optic nerve in man contains about 1,000,000 fibers. Therefore, it is important to determine how cells within the retinal network communicate and how the nerve impulses in

* Corresponding author. Tel.: (617) 496-8301; FAX: (617) 495-9300.

0165-0270/94/$07.00 © 1994 Elsevier Science B.V. All rights reserved
SSDI 0165-0270(93)E0114-H

the population of retinal ganglion cells collectively encode the visual stimulus. This requires recording the simultaneous electrical signals of many neurons.

1.2. Multi-neuronal signals

The cell bodies of the retinal ganglion cells lie in a 2-dimensional layer near the inner surface of the retina. By placing an isolated retina on a flat microelectrode array, we have succeeded in recording simultaneously the extracellular action potentials of up to 100 retinal ganglion cells in an area of 0.5 mm diameter. This represents a significant fraction of the retinal output over this region (Meister et al., 1989, 1991a). Recently, this method has been applied to study the role of spontaneous electrical activity in the development of the mammalian visual system (Meister et al., 1991; Wong et al., 1993). Here we describe extensions of this methodology to study how a population of retinal ganglion cells encodes the visual scene.

The output of the retina is carried by neurons of very diverse functional properties. Each ganglion cell is sensitive to light only in a small region of the retina, the receptive field, the center of which is generally located close to the cell body. Receptive fields of different cells vary significantly in size, shape, and spatial arrangement. The time course of the light response also varies among ganglion cells. For example, some cells are most sensitive to a rapid change in light intensity, which produces a brief burst of action potentials, whereas others can track more gradual changes in intensity by modulating their firing rate continuously. Finally, ganglion cells often differ in their sensitivity to light of various wavelengths.

Thus, the response of a retinal ganglion cell generally depends on the spatial, temporal, and spectral properties of the visual scene. These variables cannot necessarily be treated independently: for example, the time course and the spectral sensitivity of the light response often depend on spatial location within the receptive field. On the other hand, most species appear to have only a finite number of different ganglion cell types. Neurons within one functional class differ only in the spatial positions of their receptive fields. Hartline (1938) distinguished retinal ganglion cells by the sign of their response to a step change in the light intensity: ON cells fired primarily as the intensity increased, OFF cells when it decreased, and ON/OFF cells fired briefly in response to both transitions. These basic classes are found in most every retina studied to date. In addition, ganglion cells have been characterized by the time course of the response and by the degree of linear spatial summation in their receptive field. This has led to the identification of the X- and Y-types in the cat retina; both types come in the ON- and the OFF-variety. In the monkey retina, a somewhat similar subdivision into P- and M-types is now commonly accepted.

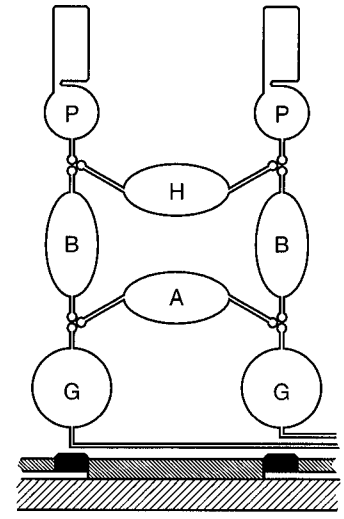

Fig. 1. Schematic diagram of the vertebrate retina on a microelectrode array, showing photoreceptors (P), horizontal cells (H), bipolar cells (B), amacrine cells (A), and ganglion cells (G).

In studying the collective activity of the ganglion cell population it is essential to recognize such basic functional distinctions between individual neurons. Cells of different types may be expected to transmit information about different aspects of the stimulus, and probably play different roles in the overall representation of the visual scene. By first identifying each neuron's receptive field and sorting the cells into smaller functional classes one can hope to reduce the combinatorial complexity of the joint firing patterns among 100 neurons.

1.3. Measuring multiple receptive fields

The common procedure for determining a ganglion cell's functional properties is tailored to single-neuron recording: One monitors the cell's firing while waving a large spot of light across the retina, thus coarsely locating the receptive field. This area is then probed more finely with a flashing spot of light, which might vary in size, intensity, flash duration, and wave length. The flashes used to probe the receptive field of one cell may not be effective in driving other ganglion cells, even those nearby. To characterize each ganglion cell recorded by the electrode array, one would have to perform this procedure sequentially, clearly an inefficient use of experimental time. Rather, one wants a stimulus that can simultaneously activate many ganglion cells to reveal their response properties. These considerations have led us to use a random flicker display. A square grid of pixels is projected onto the retina, and the color and intensity of each pixel are randomly and independently modulated in time. One

can view this as an extension of the classical method, in that the stimulus contains many small spots that flicker independently with varying frequencies and colors. Such a display has been called a "white-noise" stimulus, since it contains power at all spatial and temporal frequencies up to the cut-off frequency imposed by the display device. This stimulus elicits strong responses from most retinal ganglion cells. The recorded spike trains can then be correlated with the random stimulus sequence to determine which features of the visual display caused each ganglion cell to fire. Similar methods have been used previously to map the receptive fields of visual neurons during single-unit recording (Mizuno et al., 1985; Jones and Palmer, 1987; Reid and Shapley, 1992). As detailed below, the unbiased flicker stimulus provides a powerful tool in multi-neuron recording, as it allows a simultaneous measurement of the spatial, temporal, and spectral response properties of all the recorded ganglion cells in about 1 h.

2. Experimental methods

2.1. Preparation of the retina

Dissection and electrical recording are performed in Ringer's solution, buffered with bicarbonate, and equilibrated with a mixture of 95% O_2 and 5% CO_2. For amphibian retinae, the medium contains (in mM): 110 NaCl, 2.5 KCl, 1.6 $MgCl_2$, 1.0 $CaCl_2$, 22 $NaHCO_3$, 10 D-glucose; for mammalian retinae, the medium contains (in mM): 124 NaCl, 5 KCl, 1.15 KH_2PO_4, 1.15 $MgSO_4$, 2.5 $CaCl_2$, 25 $NaHCO_3$, 10 D-glucose. After enucleation of the eye, the eyeball is hemisected with fine scissors or a razor blade, separating the cornea and lens from the posterior half. The eyecup is rapidly drained of vitreous by inverting it on filter paper. In Ringer's, the retina is separated from the pigment epithelium with fine forceps, working from the edge of the eyecup towards the optic nerve head. Cutting the nerve allows the retina to be separated from the eyecup. Any remaining vitreous that adheres to the retinal surface is removed with tweezers. Finally, a piece about 3 mm in diameter is cut for transfer into the recording chamber described below.

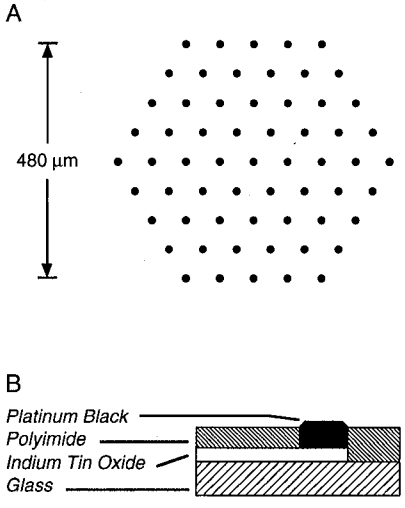

Fig. 2. A: plan view of the electrode layout. B: schematic cross-section of an electrode array, not to scale.

2.2. Electrode array

Electrical recordings were obtained with the electrode array designed by Pine and Gilbert (1982). The arrays were made at Caltech and at the Stanford Center for Integrated Systems, following procedures developed by Regehr et al. (1989). The substrate is a rectangular glass wafer with dimensions 40.4 mm × 24 mm × 0.44 mm. A region of 0.5 mm diameter at the center of the wafer bears an array of 61 passive electrodes, each 10 μm in diameter, spaced 70 μm apart (Fig. 2). Conducting leads of indium tin oxide (Gross et al., 1985) run from the electrodes to the long edges of the wafer, where contacts are made to preamplifiers. The entire surface of the wafer, except for the electrodes and the edge contacts, is insulated by a film of polyimide. To reduce the impedance of the electrodes, they are coated galvanically with platinum black (Regehr et al., 1989), resulting in a typical impedance of 100 kΩ at 1 kHz.

The electrode array pictured in Fig. 2 has a diameter comparable to the lateral range of information flow in the retina; thus it can potentially sample the results of all the neural interactions occurring in the overlying network. The electrode spacing is about 2–3 times the distance between neighboring ganglion cells in the amphibian retina or the peripheral mammalian retina. We have recently made arrays with different electrode geometries, including a linear layout of 32 × 2 electrodes spaced 60 μm apart and a dense square array of 8 × 8 electrodes spaced 30 μm apart.

2.3. Recording chamber

The glass wafer carrying the electrode array forms the bottom of a chamber that allows electrical recording from the ganglion cell layer, microscopic observation, superfusion with Ringer's, temperature control, and imaging of optical stimuli onto the photoreceptor layer (Fig. 3). A plastic ring glued onto the wafer forms the wall of the chamber. A loop of platinum wire lining the inside of this ring connects to one of the edge contacts and serves as a reference electrode. The piece of retina is transferred to the fluid-filled chamber and positioned over the electrodes with the ganglion cell layer facing down. A ring-shaped frame holding a

tightly stretched piece of dialysis membrane is then placed into the chamber over the retina. This membrane fixes the retina in place, holding the ganglion cell bodies within about 10 μm of the electrodes. It is optically transparent and very permeable (50 kDa molecular weight exclusion limit), allowing rapid exchange of ions and nutrients between the retina and the overlying pool of Ringer's medium. The frame holding the membrane rests on mylar spacers glued to the bottom of the chamber so that the retina is not compressed. The fluid in the chamber is changed continuously. Oxygenated medium flows into the chamber through glass tubing, maintaining continuous electrical contact between the fluid in the flow line and in the chamber. Fluid is removed from the other side of the chamber by suction from the surface through a beveled glass tube connected to a vacuum line via polyethylene tubing. Moistened O_2/CO_2 is blown over the top of the chamber. For work with mammalian retinae, the chamber and its surroundings are heated with a warm air gun blowing from below the electrode array. In addition, the saline is heated by passing current through a coil surrounding the inflow tubing and the temperature is monitored with a small thermistor near the bottom of the chamber. Under these conditions, one can record stable light responses from retinal ganglion cells for over 8 h.

2.4. Visual stimulation

Dynamic visual stimuli are generated on a color monitor (Apple 13″ RGB Display) driven by a computer (Apple Macintosh IIci). This image, demagnified by a factor of 80, is projected onto the retina in the recording chamber with a mirror and a 5 × objective. A glass coverslip at the top of the recording chamber provides the flat interface required to produce a sharp image on the retina. The preparation is viewed from below using an inverted microscope, taking advantage of the fact that the electrode array, except for the electrodes themselves, is optically transparent. Thus, one can focus the projected visual stimulus while simultaneously observing the retina and the electrodes. When dark adaptation is important, infrared illumination and an infrared-sensitive video camera are used to view the preparation.

The color monitor can generate a wide variety of spatial, temporal, and spectral patterns. An individual screen pixel illuminates a 5 μm spot on the retina, providing spatial resolution sufficient to stimulate single photoreceptors. The monitor's refresh rate of 67 Hz provides adequate temporal resolution for the amphibian retina, though it probably does not explore the full bandwidth of mammalian retinae (Rodieck, 1983). The monitor provides intensity contrast up to a factor

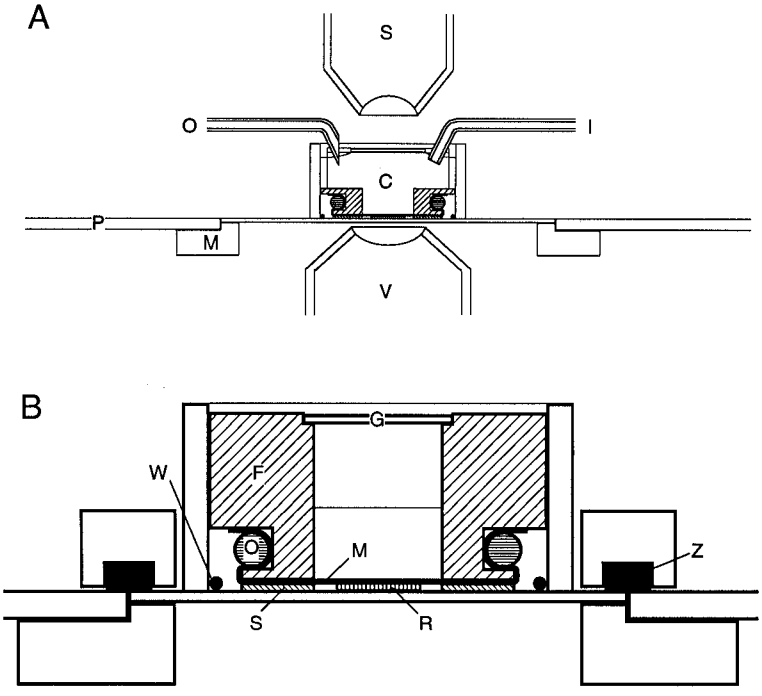

Fig. 3. A: sectional diagram of the recording chamber mounted on the stage of an inverted microscope. The electrode array forms the bottom of the chamber (C) and rests inside a rectangular cutout in the printed circuit board (P), supported by a metal frame (M). Microscope objectives are used to image the visual stimulus (S) and view the preparation from below (V). Continuous superfusion with Ringer's medium is provided through the inlet (I) and outlet (O) tubes. B: detailed section through the recording chamber perpendicular to the view in (A). A ring-shaped frame (F) with the O-ring (O) serves to stretch a piece of dialysis membrane (M). This assembly rests under its own weight on spacers (S) and holds the piece of retina (R) in place against the chamber bottom. A loop of platinum wire (W) is the reference electrode. The electrode voltage signals are transmitted from the edges of the electrode array to the adjacent printed circuit board by a strip of zebra rubber (Z).

of 200, more than the range found in most natural images. The spectral composition of the stimulus is varied by modulating the three guns of the color monitor independently. We calibrate the emission spectra of the three phosphors against the programmed gun values using a spectrophotometer (EG&G Gamma Scientific), as described by Brainard (1989).

To change the visual display instantaneously from one video frame to the next (0.015 s on this monitor), the software running the stimulator makes use of "color table animation" (Savoy, 1986): In video memory, the state of each screen pixel is determined by an 8-bit number which provides an index into a look-up table containing 256 different colors. By changing the entries of this look-up table, one can alter the screen image much more rapidly than by rewriting the contents of video memory for the entire screen. Using the Macintosh video system, this method limits the display to 254 fixed regions the gun values of which can be changed at will. Most traditional visual stimuli, such as flashing spots, moving bars, or traveling sinusoid gratings, are easily implemented within this framework. The method also lends itself to generating a random flicker stimulus for white-noise analysis. For this purpose, we display a 16×15 checkerboard of square fields. In each field, the intensity of the red gun is chosen randomly with equal probability from two levels. These levels can be chosen arbitrarily within the 8-bit resolution of the monitor; in many experiments we choose to turn the gun either off or to maximal intensity. Similarly, two further random numbers determine the state of the green gun and the blue gun, and so on for every field of the checkerboard. This produces a random checkerboard assembled from 8 possible colors. In the subsequent stimulus frame, all 720 gun settings are randomized again by drawing successive bits from a pseudorandom sequence. These pseudorandom sequences are generated by sequential calls to the *Random()* routine of the Macintosh operating system.

The size of the individual square in the flickering checkerboard determines the spatial resolution achieved in measuring the receptive field; we generally use squares of 60–100 μm width. If the 16×15 display does not completely cover the piece of retina in the chamber, it is repeated periodically in the vertical and horizontal directions. Similarly, the duration of each stimulus frame determines the temporal resolution of ganglion cell response properties. By necessity, stimulus frames are a multiple of the video frame period; we generally choose 0.015 s or 0.030 s. In these experiments, there is a direct trade-off between spatiotemporal resolution and the time required for a measurement. If the checkerboard fields are chosen too small or the stimulus frames too short, then a retinal ganglion cell will effectively average in space and time over many random stimulus values, leading to a smaller effective stimulus modulation. Thus the cell's firing rate will vary only weakly, which will necessitate a longer period of recording to achieve statistically significant measurements.

2.5. Data acquisition system

The acquisition system consists of: (1) a preamplifier board located on the microscope stage; (2) a rack-mounted box containing 61 main amplifiers and signal processors; (3) a Macintosh II computer with analog/digital interface that communicates with the signal processors and stores and displays data for on-line inspection.

The recording chamber is mounted on a printed circuit board with 61 preamplifiers. Rubber Zebra Connectors (Fujipoly, Cranford, NJ) connect the edge contacts on the wafer to corresponding traces on the printed circuit board. The voltage of each recording electrode is amplified differentially with respect to that of the reference electrode in the bath. The preamplifiers, with AC coupled inputs (0.2 s time constant) and a gain of 11, provide low-impedance output signals that pass to the main amplifiers via ribbon cable.

Fig. 4 shows signals recorded from a salamander retina by 4 electrodes. Action potentials have a typical amplitude of 100–200 μV, but range up to 500 μV. The equivalent RMS noise level at the electrode is of the order of 5 μV at a bandwidth of 2 kHz. A given action potential is often recorded on several neighboring electrodes with the spike amplitude decreasing at greater distance from the cell body. Conversely, a given electrode often records action potentials from several cells, which can be distinguished by their stereotyped amplitude and shape. Subsequent processing and analysis decompose these analog signals into spike trains from individual identified neurons. The large number of channels and the need for extended continuous

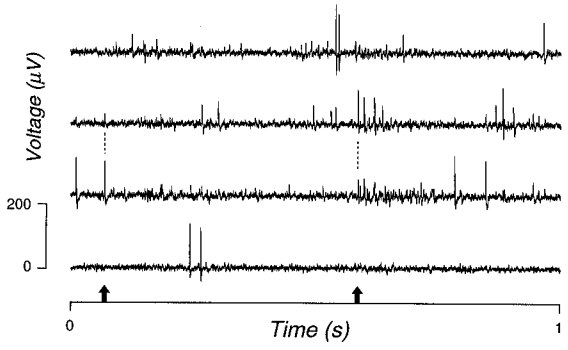

Fig. 4. Voltage traces recorded from a salamander retina by four electrodes. The arrows and dashed lines indicate individual action potentials that appear simultaneously on several electrodes. Positive voltage at the electrode is plotted downward.

recording require that the data flow be compressed at the very outset. This is achieved by 61 dedicated signal processors that extract action potentials from the analog signals in real time and describe each spike with a small set of parameters.

2.6. Signal processor

The signal processing hardware detects voltage spikes in the input signals, measures their time of occurrence, amplitude and width, and transfers these data to the computer. The amplitude and width measurements are used in subsequent analysis to distinguish the activity from different neurons recorded on the same electrode. Each signal processor channel operates independently and communicates only with the computer. The analog input signal from the preamplifier is inverted, amplified with a fixed gain of 4000, and bandpass filtered at 12 dB/octave to a bandwidth of 20–2000 Hz. This conditioned signal is available at the instrument's front panel for oscilloscope display and analog recording. At the next stage, a Schmitt-trigger circuit detects a spike when the signal crosses a preset threshold voltage (Fig. 5). This threshold is set individually for each channel with a D/A converter controlled by the computer. The time of an upward threshold crossing (time t_1) is stored temporarily by latching the lowest 8 bits of the system clock, a 24-bit ripple counter with a time unit of 50 μs. Following the upward threshold crossing, the signal is tracked by a peak detector circuit. When the signal returns below the threshold value, the lowest 8 bits of the ripple counter are latched again (time t_2). At this time, a status flag is set to indicate to the computer that a spike has been recorded on this particular channel. Simultaneously, the signal processor is temporarily disconnected from the analog voltage input, until the data for this spike are retrieved.

The computer continuously polls the status flags of all channels in a cyclic sequence, communicating through a commercial interface board (MacADIOS II, GW Instruments, Cambridge, MA). If the status flag is not set, the next channel is polled. If the flag is set, the computer performs an A/D conversion on that channel's peak detector output and reads the two bytes of time information in the latches t_1 and t_2. Then it resets the status flag and the peak detector, reconnects the signal processor to its analog input from the electrode array, and moves on to poll the next channel's status flag. Once every polling cycle, the computer also reads the highest 16 bits of the system clock to maintain continuous timing information over the duration of the experiment. In the worst case, in which all status flags are high, one cycle of polling and data transfer from all 61 channels requires ~ 0.9 ms, so the system can acquire spikes at a rate of over 1 kHz per channel. This is more than sufficient to resolve action potentials ~ 1 ms wide, as long as spikes from different neurons do not overlap in time. A 62nd auxiliary channel, identical to the others except for the absence of an amplify-

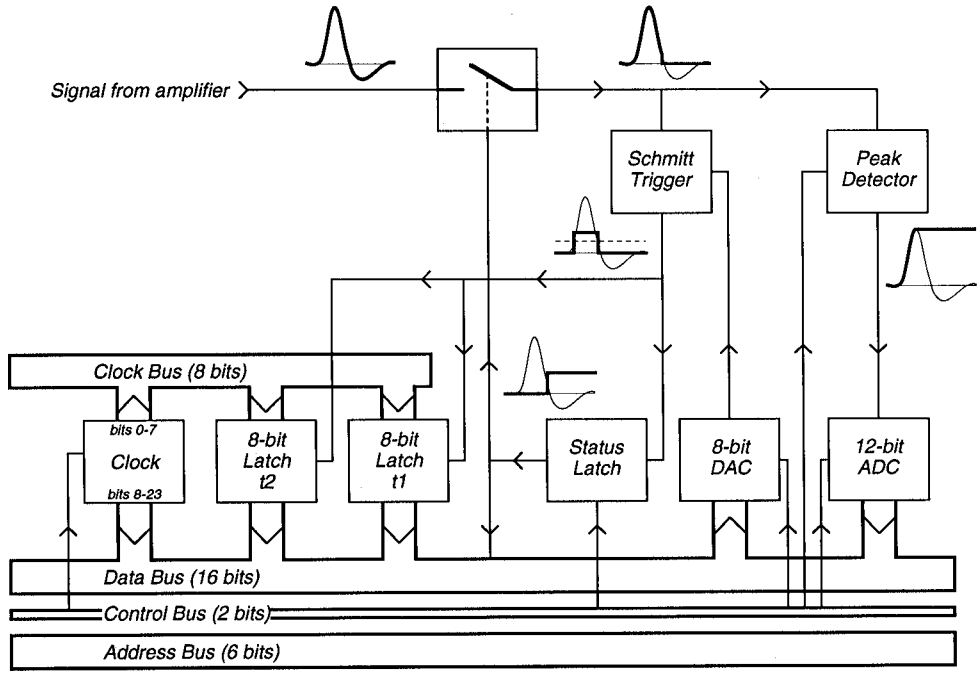

Fig. 5. Block diagram of an individual signal processor channel. See text for description. Insets show the time course of signals during acquisition of a voltage spike. The Clock and the 12-bit ADC are shared by all channels. Six address lines multiplex the signals between each channel and the data bus; these addressing components are not shown.

ing stage, is used to record signals marking external events, for example the onset of a visual stimulus sequence. A large variety of such external events can be encoded uniquely with timing pulses of different amplitude or width.

2.7. Spike acquisition software

The numbers specifying spike arrival time, amplitude, and width for each channel are stored in the computer's memory. Our current configuration allows continuous acquisition of up to 2,000,000 spikes. Periodically, recording is halted for a few seconds to write these data to hard disk. Optionally, the record can be displayed on the computer screen in the form of 61 time traces with a vertical mark denoting each action potential. On-line software provides control over the acquisition process, allowing the user to choose the set of active channels, the order in which they are scanned, and the threshold voltage for the discriminator on each channel. Typically the threshold is set just above the electrode's noise level, determined by recording from the fluid-filled chamber before mounting the retina. Finally, the recording software also triggers the optical stimulator.

2.8. Spike sorting

The first stage of off-line analysis sorts the 61 sequences of action potentials with different shapes into trains of spikes originating from single neurons and estimates the location of each neuron over the electrode array. To discriminate spikes from different cells on a given electrode, the spikes are displayed on a scatter plot of amplitude vs. width. Well-resolved action potentials in the spike train produce clusters in this display (Fig. 6). Each cluster is representative of a characteristic spike shape and can be assigned to a separate neuron.

Currently, spike sorting is performed manually, through a graphical interface with the analysis software. Since spikes from a given neuron may appear on several nearby electrodes, it is advantageous to assign the most clearly resolved action potentials first, and to remove any duplicate recordings of these spikes from the scatter plots of other channels. For this purpose, the analysis software draws a scatter plot for each channel and presents all 61 plots on the screen simultaneously. The operator picks the most prominent cluster in the display, usually the one with the largest amplitude. The set of spikes in this cluster is defined by drawing an outline around it in the width/amplitude plane. The spikes in this group are taken to be the action potentials generated by the first neuron. The program then determines whether spikes from this neuron were also recorded on other electrodes. This is

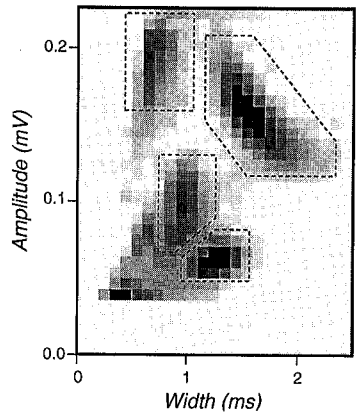

Fig. 6. Two-dimensional histogram of spike amplitude and spike width for 21250 action potentials recorded from a salamander retina by one electrode. The gray level is proportional to the number of spikes per bin. The action potentials are sorted into groups of distinct spike shape by drawing outlines separating the distinct clusters in this plot.

done by searching for precise time coincidences between spikes on other channels and spikes in the defined cluster ("crosstalk spikes"). The optimal criterion for time coincidence depends on the width of the action potentials and the average spike rate; we have typically used a ± 1 ms coincidence interval. The spikes in the defined cluster as well as their crosstalk spikes on other channels are removed from the scatter-plot displays. The user then returns to the global display of scatter plots and assigns the next best resolved cluster of action potentials. Thus, the analysis proceeds sequentially to signals of smaller and smaller amplitude. Since the lower amplitude crosstalk signals recorded on neighboring channels are removed from consideration, clusters from new neurons in the low-amplitude regime become progressively sharper. In this manner, one can eventually distinguish signals from 50 to 100 neurons. The spatial location of a neuron is estimated as the weighted average of the electrode locations where it was recorded, with each weight proportional to the respective spike amplitude. For each identified neuron, this stage of the analysis yields a spike train, consisting of a set of spike arrival times, as well as an estimate of the cell's position over the electrode array.

Further analysis refines the spike sorting.

(1) Two neurons that generate very similar spike shapes on a given channel might form a single cluster in the width/amplitude plane, and thus be defined as only one cell. This situation can be detected by computing the spike train's autocorrelation function: the average firing rate as a function of time after an action potential. If the spike train derives from a single neuron, the autocorrelation function should show an obligatory silent interval following each action potential, representing the cell's refractory period. Two or more neurons firing independently will produce a spike train

without a refractory period. In practice, the low-amplitude clusters in width/amplitude space are generally less easily resolved from each other and more likely to contain contributions from more than one neuron. Such multi-unit spike trains are still useful for certain types of analysis (Meister et al., 1991b).

(2) One neuron might generate action potentials of different shapes, thus forming two distinct clusters in width/amplitude space. This may occur when a neuron fires rapid bursts of spikes separated by only a few milliseconds. During such a burst, the spike amplitude often decreases, due to partial inactivation of the spike generating mechanism. This situation can reveal itself when two neuron definitions appear at the same computed spatial location, since spikes from the same cell will be recorded with the same amplitude ratios on neighboring channels. The occurrence of bursts can then be confirmed by crosscorrelating these two spike trains.

(3) Occasionally, the recorded spikes derive from axons. Axonal action potentials are recognizable by their characteristic triphasic waveform with an initial positive-going phase, due to outward capacitive current that depolarizes the membrane of the fiber in front of the active region. In contrast, somatic spikes begin with a negative-going phase, due to inward current at the cell body. Also, axonal spikes are considerably narrower than somatic spikes, with a typical width of only 0.3 ms. Finally, an axonal spike can usually be recorded on several electrodes along a linear trajectory traversing the array. The relatively low conduction velocity (0.4–1.0 m/s) of axons in the retina leads to characteristic distance-dependent delays in the times of spike arrival at successive electrodes. A somatic spike, on the other hand, is recorded on only 2 or 3 neighboring electrodes with no appreciable time delay. Thus, inspection of the crosstalk patterns for each defined neuron can be used to identify these signals. By these criteria, we estimate that about 5% of our recorded action potentials represent axonal spikes.

Inspecting a record of the full original wave forms often helps to classify spikes of dubious origin. For this purpose, the amplified and filtered analog signals are stored on an 8-channel digital recorder (Neurodata DR-890), which successively collects signals from all 61 electrodes over the course of an experiment.

2.9. Spike train analysis

The choice of analysis methods applied to the recorded spike trains depends entirely on the experimental design. Most classical studies of sensory processing adopt a "forward" approach: one presents a defined stimulus, such as a flash of light, repeats this stimulus many times, and analyzes the statistics of the resulting spike trains. In this way, one can estimate the likelihood of obtaining any neuronal output signal given the specified sensory input. In practice, such computations have most often been limited to the first and second moments of the spike trains. The mean firing rate of a neuron is estimated by constructing a histogram of the times of occurrence of spikes, averaged over many stimulus cycles (see Fig. 7). Similarly, the probability for joint firing of two neurons is estimated by a 2-dimensional histogram of spike times from both cells. These methods are widely used (for review see Glaser and Ruchkin, 1976).

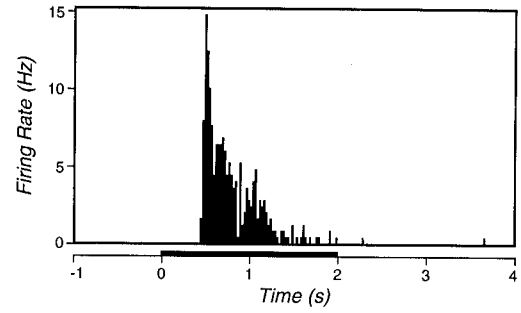

Fig. 7. Response of a salamander ganglion cell to a spatially uniform light flash of 2 s duration. The plot shows the cell's firing rate as a function of time, averaged over 100 presentations of the flash, the duration of which is indicated by the black bar.

An alternative is the "reverse" approach, where one presents the system with a great variety of stimuli, each presented only once. One then specifies a defined neuronal response, such as an action potential, and analyzes the distribution of all stimuli that caused this response. In this way, one can estimate the likelihood of any input stimulus given observation of the specified neuronal output. We use such a technique to analyze the responses to white-noise flicker stimulation. The goal of these experiments is to determine the receptive field of each recorded neuron. For a given cell, one first determines which segments of the random stimulus sequence elicited an action potential. Since the overall integration time of the retina is generally less than 1 s, we limit the analysis to the stimulus segment of 1 s duration preceding each action potential. The set of all such random sequences of video frames ending in an action potential is called the "spike-triggered stimulus ensemble". These are the sequences that the neuron under study has flagged as "interesting" by firing an action potential. To determine what all these sequences have in common, one computes the average over this ensemble, also called the "spike-triggered average stimulus". As illustrated in Fig. 8, this is the average visual stimulus sequence presented to the

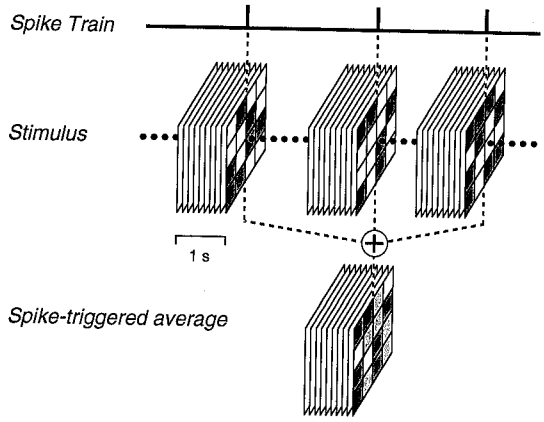

Fig. 8. Spike-triggered averaging of the random checkerboard stimulus. Only a 4×4 section of the checkerboard is shown. Each stack of frames represents the 1-s stimulus sequence preceding an action potential. These sequences are then aligned and averaged.

retina during the 1 s interval preceding an action potential from the selected neuron. Formally, if

$S_t^{(h,v,g)}$

= light intensity of gun g in the display pixel (h,v) during time bin t of the experiment

N_t = number of spikes recorded during time bin t

then

$\bar{S}_t^{(h,v,g)}$

= spike-triggered average intensity of gun g in pixel (h,v) at time t relative to a spike

$$= \frac{\sum_{t'} N_{t'} S_{t'+t}^{(h,v,g)}}{\sum_{t'} N_{t'}}$$

For each gun, these values range between the low- and high-intensity levels chosen during flicker stimulation. The spatial, temporal, and spectral properties of this spike-triggered average stimulus are a measure of the stimulus features effective for exciting this cell.

3. Examples

3.1. The population response to a flash of light

In an early experiment, we surveyed the variety of light responses among ganglion cells in the retina of the tiger salamander (*Ambystoma tigrinum*). The dark-adapted retina was stimulated with a uniform pulse of white light lasting 2 s. This stimulus was repeated 100 times at 10 s intervals. Fifty neurons were identified from the recorded signals. Fig. 7 illustrates the average light response of one cell with a histogram of spike times relative to the onset of illumination, pooled over 100 stimulus presentations. The ordinate is scaled to show the cell's average firing rate. This ganglion cell was silent in darkness, but began firing with a delay of ~0.4 s after the light was turned on. The firing rate then decreased gradually, and activity ceased even before the light was turned off.

Fig. 9 shows the light responses of 12 different neurons, plotted as in Fig. 7, along with the cell locations. This small region of retina contained ganglion cells with widely varying response properties. Some cells responded transiently to an increase of illumination, others to a decrease, and still others fired tonically while the light was on or while the light was off. This variety of responses is expected if each region of the retina represents many features of the local light pattern.

3.2. Measurement of a receptive field

Fig. 10 illustrates a ganglion cell's receptive field, as determined by a white-noise flicker experiment. The

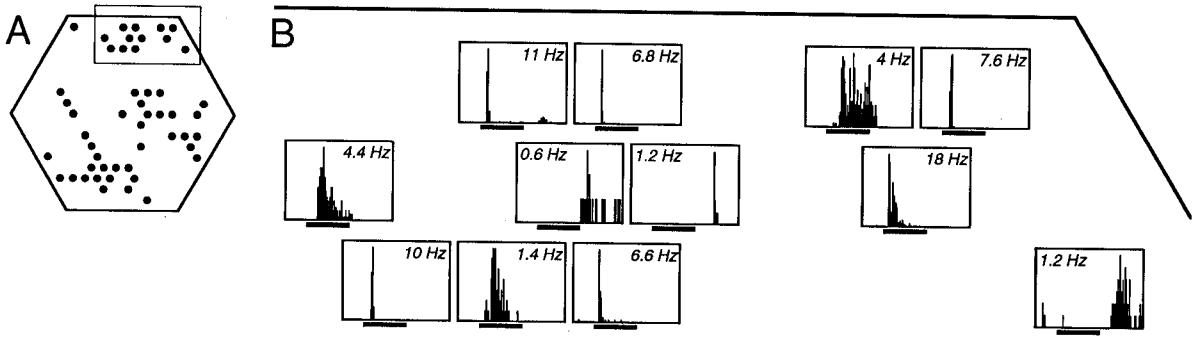

Fig. 9. A: locations, relative to the electrode array, of 50 identified ganglion cells in one preparation. B: light responses of 12 ganglion cells in the upper right hand region of (A). The plots show the average firing rate as a function of time relative to a 2 s light flash, indicated by the bar. Each plot is scaled to the maximal firing rate, indicated at the top.

retina was stimulated with a flickering checkerboard the individual fields of which measured 75 μm on a side, and the gun intensity values of which were changed randomly every 15 ms. During 4300 s of recording, the cell illustrated here generated 9738 action potentials. From this spike train and the known stimulus sequence, the spike-triggered average stimulus was computed, as described above. Fig. 10A shows a single frame from this time sequence, namely the average image on the retina 0.155 s before the neuron fired a spike. There is an elongated bright region, close to the location of the cell body. The time course of the intensity within that region, termed the "center", is plotted at the top of Fig. 10B. For each gun, these intensity values are normalized such that +1 and −1 correspond, respectively, to the high- and low-intensity levels chosen for flicker stimulation; on this scale, the time-averaged stimulus value is zero for each gun. Moving backward in time from the action potential, the spike-triggered average intensity increases from zero (average) to a peak (brighter than average) at −0.15 s, then drops into an undershoot (dimmer than average) before settling at the zero baseline. One concludes that the cell was excited by light within the bright elongated region. It responded by firing an action potential on average about 0.15 s later. The undershoot indicates that the cell was excited most efficiently by a positive transition from dimmer to brighter light. Finally, one sees that the red and green guns were about twice as effective as the blue gun, suggesting that the cell's sensitivity peaked in the yellow region of the visual spectrum. From the emission spectra of the color monitor and the known absorption spectra of salamander photoreceptors we find that these ratios of sensitivities are consistent with a dominant input to the ganglion cell from the red-sensitive cone photoreceptors.

The cell was also sensitive to light outside the center region. In the surround, it was excited by a decrease in light intensity, a sensitivity opposite to that of the center. Note that light in the surround acted with a somewhat longer delay. The peak of the spike-triggered average occurs at about −0.20 s, probably reflecting additional processing delays in the horizontal cell layer. Although individual pixels in the surround were much less effective at generating spikes than pixels in the center, the overall contribution of the surround to the cell's response was about 83% that of the center.

By using a stimulus that is richly modulated in the spatial, temporal, and spectral domains, one can thus measure the ganglion cell's functional properties in all these dimensions. The analysis can be performed for every recorded neuron to assess the functional composition of the ganglion cell population. Further studies building on this approach my help to reveal how the concerted activity in this heterogeneous population of neurons encodes a complex visual image for transmission to the brain.

4. Discussion

We have described a new experimental method for the study of multi-neuronal signaling in the vertebrate retina. The essential components are: visual stimulation of the photoreceptor layer with a color monitor; parallel recording from 61 sites of a multi-electrode array; detection and acquisition of action potentials by a 62-channel hardware recorder; off-line spike sorting resulting in separate spike trains from up to 100 neurons; and reverse correlation analysis to measure single-neuron response properties. Although many of

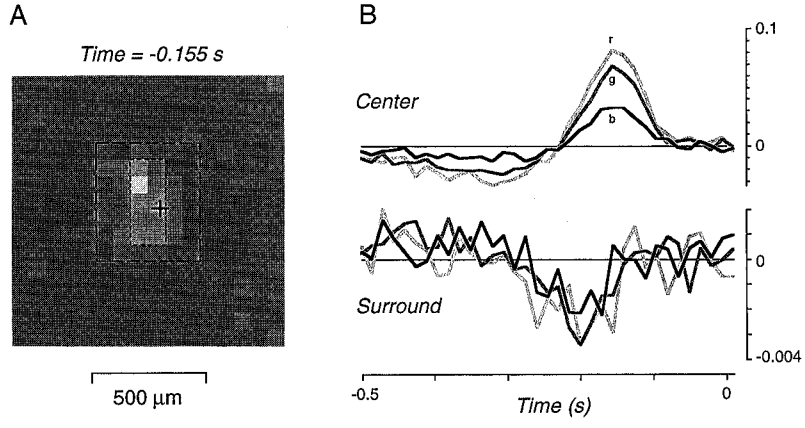

Fig. 10. Receptive field of a salamander retinal ganglion cell, as determined from random checkerboard stimulation. A: the spike-triggered average stimulus 155 ms before the action potential. The electrical recording location is marked by a cross. B: time course of the spike-triggered average intensity, computed independently for the red, green, and blue guns, and averaged over all display pixels within the inner outline in (A) (Center), and over all pixels outside the outer outline (Surround). On the ordinate, +1 and −1 correspond respectively to the high and low gun intensities used during flicker stimulation.

these tools have been used previously, their integrated application provides unique experimental access to a large neuronal circuit. One can apply the retina's natural stimulus throughout its entire dynamic range, and simultaneously monitor a large fraction of the resulting neural response. Such measurements should be useful in analyzing how retinal neurons collectively process and encode visual information. Below, we comment briefly on general strategies for multi-neuronal recording and analysis.

4.1. Multi-neuronal recording

Previously reported schemes for multi-electrode recording have emphasized the on-line sorting of action potentials. For example, in the system described by Gerstein et al. (1983), the experimenter acquires a small sample of spikes and sets the criteria for spike sorting, analogous to the cluster outlines in Fig. 6. Subsequently, the acquisition system uses these criteria to sort the spikes in real time. The user continuously monitors the performance of the sorters to guard against slow drifts in the spike shapes. While this approach may be useful when recording from a handful of electrodes, it is probably not feasible to monitor 100 or more spike sorters in this way. It is also not necessary for the experimenter to get immediate feedback about each individual spike train, as there is little hope of understanding the intricacies of concerted firing patterns of 100 neurons in real time. We have instead adopted a strategy for data acquisition similar to that in particle physics experiments: real-time electronics are used to compress the data rate by acquiring only interesting events, here action potentials, and describing each event with accuracy sufficient for a unique identification. The interpretation of such events is left to off-line analysis, which typically takes very much longer than the experiment itself. Our acquisition system measures two spike parameters, amplitude and width, that are widely used shape discriminators. The additional data compression that could be achieved by instantly sorting the spikes and discarding the shape parameters is not essential. The implementation of this system in hardware has proven very robust, operating maintenance-free for the past 4 years. As the design requires only few electronic components per channel, it is suitable for future expansion to more electrodes.

4.2. White-noise stimulation and analysis

The random flicker display used in our experiments efficiently explores the space of all visual stimuli along the dimensions of space, time, and wave length. Thus it can elicit responses simultaneously from many ganglion cells that differ in their receptive field locations and other response properties. Such stimuli also have a special role in white-noise analysis (Marmarelis and Marmarelis, 1978; Sakai et al., 1988). In this formalism, one expresses the neural system's output, for example the firing rate of a retinal ganglion cell, as a functional power series of its input, for example the time-dependent distribution of light intensity. By performing experiments with an input that is perfectly uncorrelated in time, such as a random flicker stimulus, one can compute the various kernels in this expansion as correlation functions between the input and the output. For example, the spike-triggered average stimulus, $\overline{S}_t^{(i,j,g)}$, is proportional to the time-reverse of the first-order kernel relating the light intensity to the ganglion cell's firing rate. If the ganglion cell's light response were purely a linear function of the light intensity on the retina, this first-order kernel would provide a complete description of the cell's response properties. Under this condition of linearity, one can show that the firing rate in response to a brief flash of one gun in one field of the checkerboard is proportional to the time-reverse of the corresponding spike-triggered average, that is

$$\overline{N}_t = \text{average number of spikes in time bin } t \text{ following a flash of gun } g \text{ in pixel } (i,j) = c \cdot \overline{S}_{-t}^{(i,j,g)}$$

Clearly, however, the retina is not a purely linear system. For example, many ganglion cells respond well to a step in light intensity of either sign. Thus, the spike-triggered average stimulus is generally not a complete description of all aspects of the neuron's response. Nevertheless, among several hundred examples we have never observed a neuron that was driven by light flashes but failed to generate a significant spike-triggered average. Apparently, all retinal ganglion cells have a strong linear component to their light response. Whether this linear component suffices to fully distinguish the major functional response types remains to be determined.

One could extract higher-order kernels of the response function by computing the correlation of the firing rate with higher powers of the visual stimulus. In fact, the white-noise approach has been praised because, in principle, a single experiment can reveal all aspects of the stimulus-response relationship, as long as the reverse correlation analysis is carried to a sufficiently high degree. Though such a systematic expansion is enticing in theory, it has not been particularly useful in practice. In neurophysiology few attempts have been made to compute such reverse correlations beyond the second order. The exercise fails mostly due to the vast number of terms that appear in the functional expansion: The n^{th} order kernel relating a single response variable to N_S stimulus variables is composed of $(N_S N_T)^n$ terms, where N_T is the number of time bins of stimulus history included in the expansion. The

problem is particularly severe in visual studies due to the large number of independent variables needed to specify the spatial, temporal, and spectral dimensions of the visual stimulus. Analyzing multi-neuronal activity exacerbates the situation. Now the firing rates of different neurons cannot be treated as independent response variables. Thus a complete correlation analysis must include higher-order products of the recorded spike trains as well as higher powers of the stimulus. For a typical neuronal circuit such as the retina, the number of possible reverse correlation functions of higher than first order is daunting. Therefore, it appears that the unbiased "black box" approach derived from systems analysis will not be very helpful when dealing with neuronal circuits of even moderate size. Faced with the combinatorial complexity of many input and output variables, one will need to carefully choose which aspects of multi-neuronal activity to analyze. These choices should be guided by a thorough understanding of the neuronal system at both lower and higher levels of integration: the functional properties of the circuit's individual component neurons, but also the role the circuit plays in the overall behavior of the organism. As the technical problems of observing multi-neuronal activity are being overcome, the development of a conceptual framework and analytical tools for its interpretation has a high priority for our understanding of neuronal systems.

5. Acknowledgements

We would like to acknowledge the help of Dr. Alan Litke, Robert Schneeveis, and Chris Ziomkowski. This work was supported by a grant from the Lucille P. Markey Charitable Trust to M.M., Grant 238c from the Systems Development Foundation and NIH Biomedical Research Support Grant RR07003 to J.P., and Grant EY 05750 from the National Eye Institute, USPHS, and an award from the Retina Research Foundation to D.A.B.

6. References

Brainard, D. (1989) Calibration of a Computer Controlled Color Monitor, Color Res. Appl., 14: 23–34.

Dowling, J.E. (1987) The Retina: an Approachable Part of the Brain, Harvard University Press, Cambridge, MA.

Gerstein, G.L., Bloom, M.J., Espinosa, I.E., Evanczuk, S. and Turner, M.R. (1983) Design of a Laboratory for Multineuron Studies, IEEE Trans. Syst. Man Cybern., SMC-13: 668–676.

Glaser, E.M. and Ruchkin, D.S. (1976) Principles of Neurobiological Signal Analysis, Academic Press, New York.

Gross, G.W., Wen, W.Y. and Lin, J.W. (1985) Transparent indium-tin oxide electrode patterns for extracellular multisite recordings in neuronal cultures, J. Neurosci. Methods, 15: 243–252.

Hartline, H.K. (1938) The response of single optic nerve fibers of the vertebrate eye to illumination of the retina, Am. J. Physiol., 121: 400–415.

Jones, J.P. and Palmer, L.A. (1987) The two-dimensional structure of simple receptive fields in cat striate cortex, J. Neurophysiol., 58: 1187–1211.

Levick, W.R. and Dvorak, D.R. (1986) The retina – from molecules to networks, TINS, 9: 181–185.

Marmarelis, P.Z. and Marmarelis, V.Z. (1978) Analysis of Physiological Systems: The White-Noise Approach, Plenum Press, New York.

Meister, M., Lagnado, L. and Baylor, D.A. (1991a) Multineuronal signalling by retinal ganglion cells, Soc. Neurosci. Abst., 17: 344.

Meister, M., Pine, J. and Baylor, D.A. (1989) Multielectrode recording from the vertebrate retina, Invest. Ophthalmol. Vis. Sci., 30 (Suppl.): 68.

Meister, M., Wong, R.O.L., Baylor, D.A. and Shatz, C.J. (1991b) Synchronous bursts of action potentials in ganglion cells of the developing mammalian retina, Science, 252: 939–943.

Mizuno, M., Imai, S., Tsukada, M., Hida, E. and Naka, K.-I. (1985) A micro-computer system for spatio-temporal visual receptive field analysis, IEEE Trans. BME, 32: 56–59.

Pine, J. and Gilbert, J. (1982) Studies of cultured cells in dishes incorporating integral microcircuit electrodes, Soc. Neurosci. Abst., 8: 670.

Regehr, W.G., Pine, J., Cohan, C.S., Mischke, M.D. and Tank, D.W. (1989) Sealing cultured invertebrate neurons to embedded dish electrodes facilitates long-term stimulation and recording, J. Neurosci. Methods, 30: 91–106.

Reid, R.C. and Shapley, R.M. (1992) Spatial structure of cone inputs to receptive fields in primate lateral geniculate nucleus, Nature, 356: 716–718.

Rodieck, R. (1973) The Vertebrate Retina, W.H. Freeman Press, San Francisco.

Rodieck, R.W. (1983) Raster-based colour stimulators, In: J.D. Mollon and L.D. Sharpe (Eds.), Colour Vision Physiology and Psychophysics, Academic Press, London, pp. 131–144.

Sakai, H.M., Naka, K.-I. and Korenberg, M.J. (1988) White-noise analysis in visual neuroscience, Vis. Neurosci., 1: 287–296.

Savoy, R.L. (1986) Making quantized images appear smooth: tricks of the trade in vision research, Behav. Res. Methods, Instruments, Computers, 18: 507–517.

Wong, R.O.L., Meister, M. and Shatz, C.J. (1993) Transient period of correlated bursting activity during development of the mammalian retina, Neuron, 11: 923–938.